Supporting information

A Sensitive SERS Assay of Protein and Nucleic Acid using Triple-Helix Molecular Switch for Cascade Signal Amplification

Sujuan Ye,[ab] Yanying Wu,[b] Wen Zhang,[a] Na Li [a] and Bo Tang*[a]

[a] *College of Chemistry, Chemical Engineering and Materials Science, Collaborative Innovation Center of Functionalized Probes for Chemical Imaging, Key Laboratory of Molecular and Nano Probes, Ministry of Education, Shandong Normal University, Jinan 250014, P. R. China*

[b] *College of Chemistry and Molecular Engineering, Qingdao University of Science and Technology, Qingdao 266042, China*

*E-mail: tangb@sdnu.edu.cn

Table of Contents

Experimental section

Reagents. All oligonucletides used in the present study were purchased by Sangon Biotech Co., Ltd. (Shanghai China) and listed in Table S-1. The Klenow Fragment of DNA Polymerase I (KF polymerase), E.coli (10 U/μL) and the deoxynucleotide solution mixture (dNTPs) were ordered from TaKaRa Bio-technology (Dalian) Co.,Ltd. Nb.BbvCI (10 U/μL) was obtained from New England Biolabs (Beijing). Coralyne (CORA), 1-Ethyl-3-(3-dimethylaminopropyl) carbodiimide (EDC), and N-hydroxysuccinimide (NHS) were purchased from Sigma-Aldrich. $HAuCl_4 \cdot 4H_2O$ was ordered from Shanghai Reagent Co., Ltd. (Shanghai, China). Carboxyl-modified magnetic beads (MBs, 1.0-2.0 μm, 10 mg/mL) were purchased from BaseLine ChromTech Research Centre, China. All other reagents were of analytical reagent grade. All the water used in the work was RNase-free.

Apparatus. UV/Vis absorption spectra were obtained with a Cary 50 Series Spectrophotometer (Varian, Australia). Raman measurements were conducted in a Renisaw Invia Raman spectrometer (RamLab-010) at an excitation laser of 633 nm. A microscope equipped with a 50 × objective was used to focus the incident excitation laser. The laser power on the sample was 5 mW, and the accumulation time was 10 s. The Raman spectrometer was calibrated with WiRE Raman Software Version 2.0 (Renisaw Ltd.) Transmission electron microscopy (TEM) images were recorded on a JEM 1200EX trans-mission electron microscope (JEOL, Japan). Fluorescence spectra were measured using a Hitachi F-4600 fluorescence spectrometer (Hitachi Ltd., Japan)controlled by FL Solution software.

Synthesis of gold nanoparticles: Gold nanoparticles (AuNPs) were synthesized by the reduction of tetrachloroauric acid ($HAuCl_4$) with trisodium citrate following the published protocols.[1,2] Briefly, after boiling the $HAuCl_4$ solution (0.01% (w/w), 50 mL) under vigorous stirring, 0.75 mL of 1% (w/w) trisodium citrate solution was added to the solution rapidly and stirred for 30 min at the boiling point. The color change of the solution from faint yellow to purple indicates the formation of AuNPs. With continuous stirring, the solution was cooled naturally to room temperature and the prepared AuNPs were

characterized by TEM (Figure S-1). The obtained gold colloidal solution was stored in brown glass at 4 °C until use.

Preparation of SERS signal probe: The process of AuNPs functionalized SERS signal probe was performed as follows.[3,4] Briefly, 50 μL of 1×10^{-7} M signal DNA (5'-thiol, 3'-Rox) and 10 μL of 1×10^{-8} M capture DNA (5'-thiol) were activated with acetate buffer (pH 5.2) and 1.5 μL of 10 mM TCEP for 1 h, then they were added to freshly prepared AuNPs (1 mL), and shaken gently at 37 °C for 16 h. Then, the solution was aged in salts (0.05 M NaCl, 200 μL) for 6 h and in salts (0.1 M NaCl, 200 μL) for 6 h, respectively. Excess reagents were removed by centrifuging at 15000 rpm for 30 min. The red precipitate was washed and centrifuged repeatedly for three times. The resulting SERS signal probe was finally dispersed into 100 μL 0.01 M phosphate buffer solution (PBS, 0.01 M KH_2PO_4/ K_2HPO_4, pH 7.4, 0.1 M NaCl) and stored at 4 °C.

Immobilization of hairpin DNA onto MB: Coupling the hairpin DNA onto the surface of MB was performed according to the reference with a slight modification.[5] First, 100 μL suspension of carboxylated MBs was placed in a 0.5 mL Eppendorf tube (EP tube) and separated from the solution on a magnetic rack. After washed with imidazol-HCl buffer (pH 6.8, 0.1 M, 200 μL) for three times, MBs were activated in 200 μL of o.1 M imidazol-HCl buffer (pH 6.8) containing 0.1 M EDC at 37 °C for 30 min. After MBs were washed with 200 μL 0.01 M PBS (pH 7.4, 0.3 M NaCl) three times, 200 μL amino group modification hairpin DNA were separately added to the above freshly activated MBs and incubated at 37 °C overnight. Finally, the excess DNA was removed by magnetic separation. The resulting hairpin DNA conjugated MBs were rinsed three times with 200 μL of 0.01 M PBS (pH 7.4), redispersed in 200 μL of 0.01 M PBS and stored at 4 °C for use.

Fabrication of THM. The fabrication of triple-helix configuration was conducted according to the literatures. [6,7] Trigger DNA (10^{-6} M, 200 μL) and Triple-helix DNA binding molecules (CORA, 5×10^{-6} M, 200 μL) were added into the prepared hairpin DNA and incubated for 1 h at 37 °C. The resultant triple-helix conjugated MBs were washed with PBS for three times, then redispersed in 200 μL of 0.01 M PBS and stored at 4 °C for future use.

Fluorescence measurement of the formation of the THM. All fluorescence measurement was performed with F-4600 FL spectrometer. The instrument settings were chosen as follows: λex = 470 nm (slit 5 nm), λem =518 nm (slit 5 nm), PMT detector voltage = 700 V.

The assay procedure of lysozyme and p53 target DNA. For lysozyme detection (the immobilization of hairpin DNA onto MB in the Supporting Information), different concentrations of lysozyme (5 μL) were added to the solution mixed with DNA-MB complex suspension (5 μL), SERS signal probes (10 μL), Klenow polymerase (0.3 $UμL^{-1}$), dNTPs (6 μL) and Nb.BbvCI (0.4 $UμL^{-1}$). After incubated at 37 °C for 1.5 h, the mixture was heated at 80 °C for 20 min to inactivate the enzymes and cooled at 37 °C for 20 min. After that, the MBs anchored SERS signal probes were performed through magnetically controlled separation to remove the excess SERS signal probes, washed with PBS for three times and redispersed in 50 μL of 0.01 M PBS. During the evaluation of the sensitivity and specificity for p53 target DNA, the selected biomolecules (e.g., nontarget molecules and p53 target DNA) were used as analytes, and the experiments were conducted according to the method described above.

Measurement of SERS. 2 μL MBs suspension was casted on Au slices and air-dried at room temperature. Raman spectrum was obtained by using a Renisaw in Via Raman spectrometer (RamLab-010) at an excitation laser of 633 nm. The laser power was 5 mW, and the resolution of SERS spectra was over cm^{-1}. The acquisition time for each spectrum was 10 s. Three spectra were obtained from different cites of each sample and averaged to represent the SERS results, and three repeated experiments were carried out. Error bars showed the standard deviation of the three experiments.

Characterization of AuNPs

The prepared AuNPs were characterized by TEM (Figure S-1).

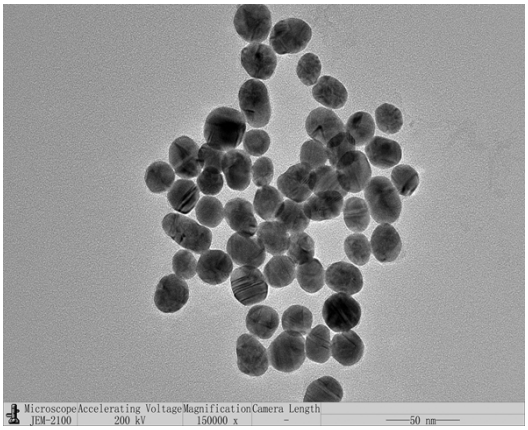

Figure S-1. TEM image of AuNPs synthesized (about 24.5 nm)

UV-visible spectra of the Rox-DNA conjugates

The UV-visible spectra of signal probe (Rox-DNA), capture probe, AuNPs and SERS bio-bar codes (SERS signal probes) were carried out on a Cary 50 UV/Vis-NIR spectrophotometer. As shown in Figure S-2, the curve a, b, c exhibited the characteristic absorbance of AuNPs (~520 nm), capture DNA (~260 nm) and Rox-DNA (~260 nm and two characteristic absorbance at 500~600 nm, respectively, consistent with the literature [8]). Curve d exhibited both the characteristic absorbance of Rox-DNA and AuNPs, indicating the successful conjugation of Rox-DNA with AuNPs.

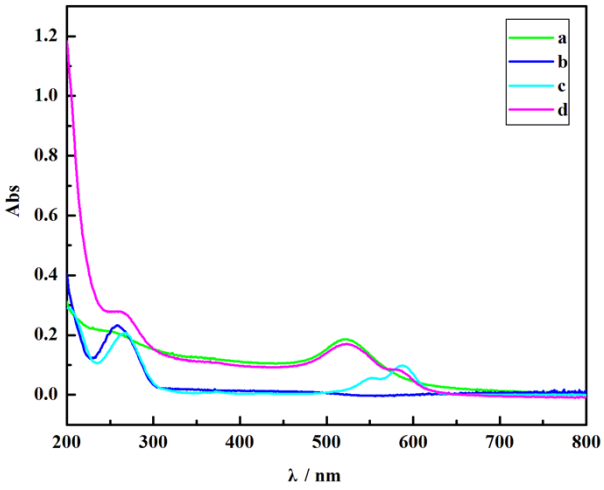

Figure S-2. UV spectra of Au colloid (a), DNA (b), Rox-DNA (c), and bio barcode DNA (d)

The structure of Rox

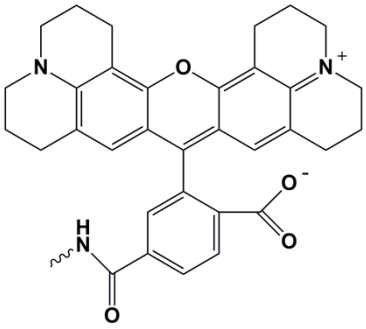

Characterization of the formation of THM

A series of control experiments were carried out. The results were shown in Figure S-3. In the presence of hairpin DNA labled with FAM (curve a), the fluorescence intensity was relatively high. In the presence of hairpin DNA and noncomplementary trigger DNA labeled with DABCYL, the fluorescence intensity was decreased (curve b), due to that the quencher can partly quench the fluorescence signal. In the presence of hairpin DNA, complementary trigger DNA and the triplex binder, the complementary trigger DNA can hybridize with hairpin DNA to diminish the distance between fluorophore and quencher. So the triple-helix molecule was formed. It is understandable that the fluorescence intensity was dramatically decreased (curve c),which was similar to the PBS buffer solution (curve d). According to the result of fluorescent characterization, we can demonstrate that triple-helix molecule was fabricated successfully.

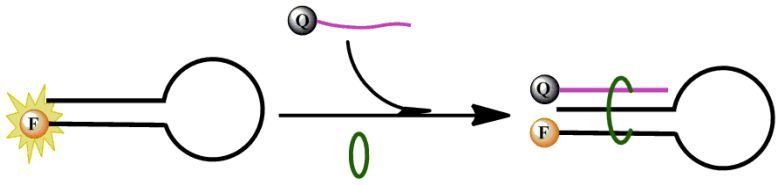

Scheme S-1. The schematic representation of the formation of THM.

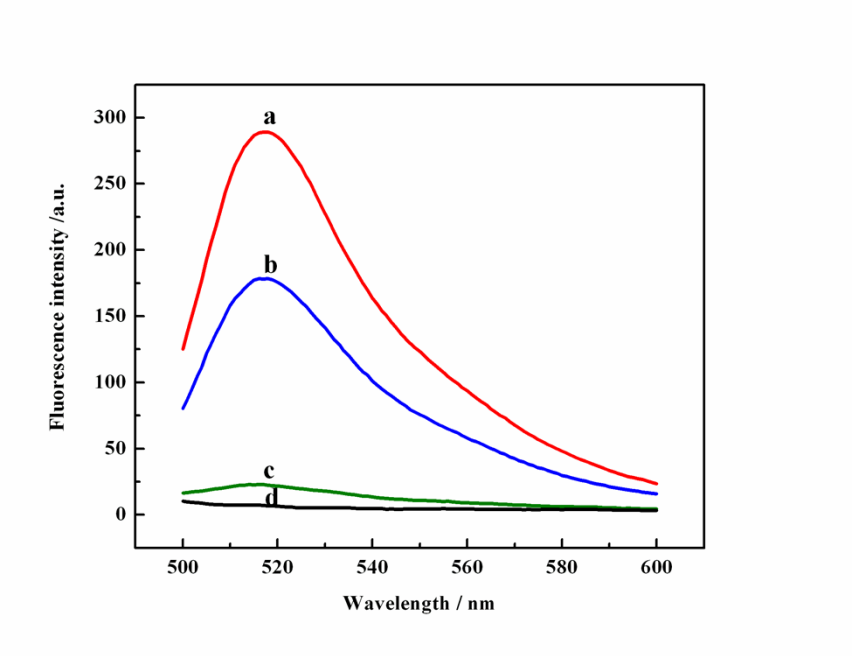

Figure S-3. Fluorescence responses of hairpin DNA labled with FAM(a), hairpin DNA labled with FAM and noncomplementary trigger DNA labeled with DABCYL (b), hairpin DNA labled with FAM, complementary trigger DNA labeled with DABCYL and the triplex binder (c), and the PBS buffer solution (d)

Optimization of the experimental conditions

Optimization of the triple-helix DNA hybridization: The concentration of salt in the reaction solution and triple-helix DNA hybridization time are two important factors for the fabrication of triple-helix configuration. Figure S-4A depicted the variation of Raman intensity at different concentrations of NaCl. Based on the result, 0.3 M NaCl was used for the triple-helix DNA hybridization. Figure S-4B showed that the Raman intensity reached the maximum at 60 min and then changed little. That is, the hybridization time for the formation of the triple-helix configuration was 60 min.

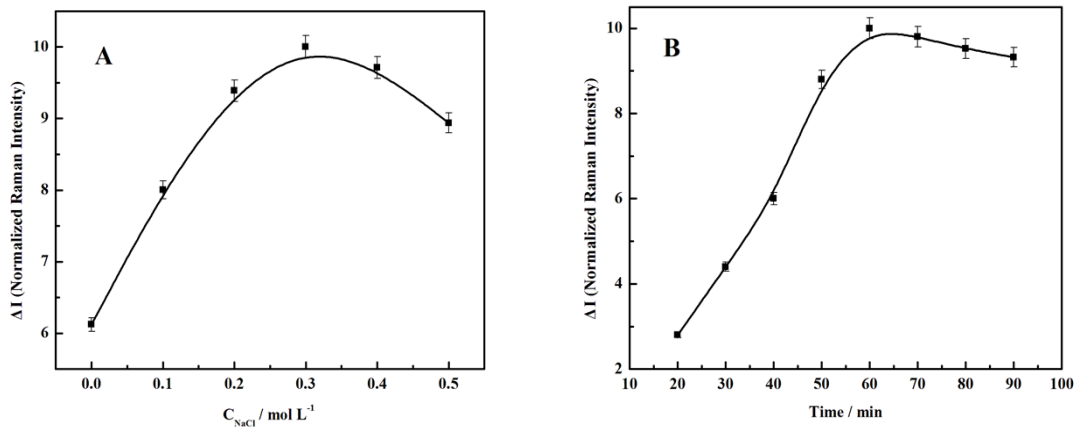

Figure S-4. Effect of the concentration of NaCl (A) and the time of triplex DNA hybridization (B) on the normalized Raman signal.

Optimization of the reaction temperature and pH: The reaction temperature and pH of PBS has an important influences on DNA hybridization and enzyme bioactivity, the most two important parameters to optimize the analysis system. We investigated the intensity of Raman detection under different temperature and pH conditions. Figure S-5A showed the influence of pH on the Raman intensity produced by 1.0×10^{-13} M lysozyme. A maximal Raman intensity (ΔI) was obtained at pH 7.4. We therefore selected pH 7.4 as the optimical condition.

The intensity of Raman detection under different temperature conditions was investigated. As shown in Figure S-5B, the Raman intensity (ΔI) increased with increasing temperature from 20 °C to 37 °C. A maximum is reached at 37 °C, followed by a gradual decreased. Obviously, 37 °C was chosen as the optimal temperature.

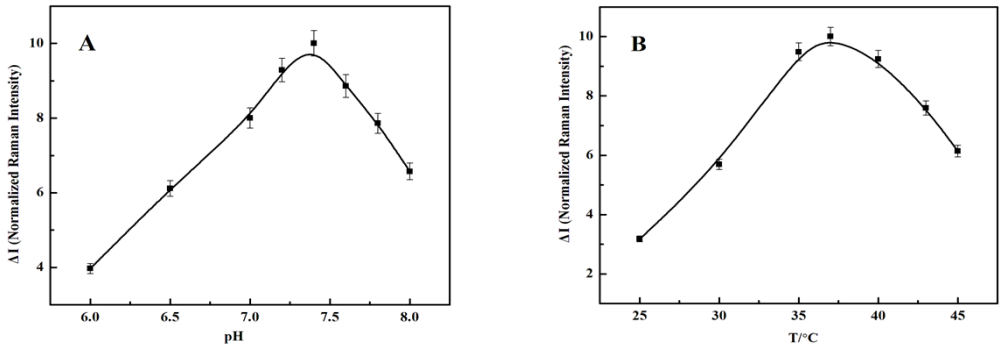

Figure S-5. Influence of pH (A) and temperature (B) of the reaction, on the ΔI signal responding to 10^{-13} M lysozyme.

Optimization of the amount of KF polymerase and nicking endonuclease: The amount of KF polymerase and nicking endonuclease have also effected on the Raman intensity. To improve the sensitivity of Raman detection, we designed a series of control experiments to optimize the amount of KF polymerase and Nb.BbvCI. The results showed that the Raman intensities increased rapidly with the increase of the amount of the polymerase up to 0.3 $UμL^{-1}$, followed by a plateau. Hence 0.3 $UμL^{-1}$ of KF polymerase was adopted to be the optimum amount for the system polymerization. Similarly, as it could be seen in Figure S-6, 0.4 $UμL^{-1}$ of Nb.BbvCI was the optimum.

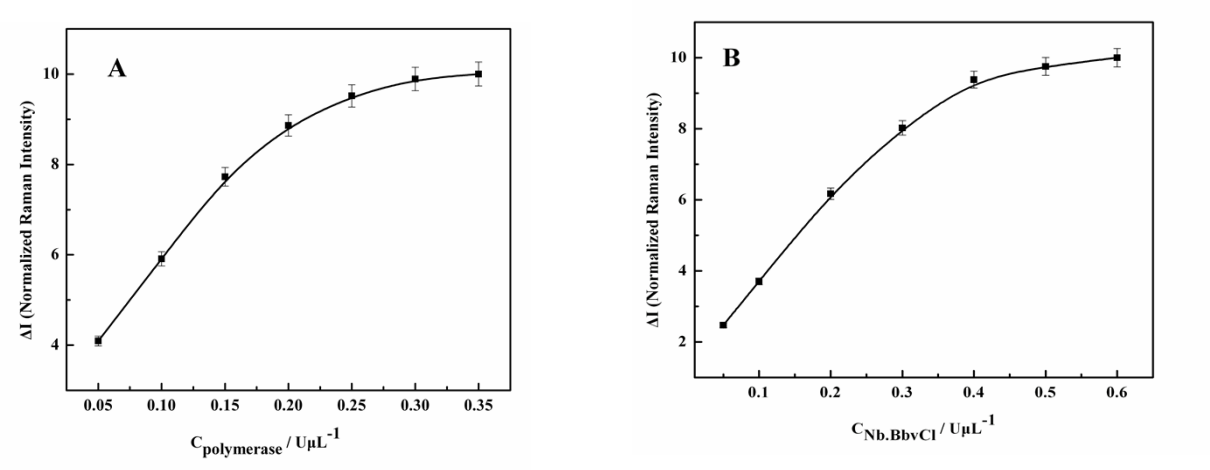

Figure S-6. Effect of the amount of KF polymerase (A) and Nb.BbvCI (B) on the ΔI signal responding to 10^{-13} M lysozyme.

Optimization of the incubation time: In order to achieve the best sensing performance, the incubation time was investigated by performing the experiment at different time intervals. The results (Figure S-7) revealed that the Raman intensity increased rapidly with the prolonging incubation time and nearly reached a plateau after 90 min. Therefore, the reaction time was kept at 90 min in the experiment.

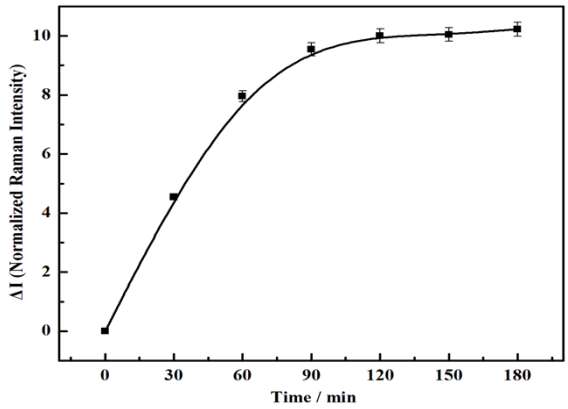

Figure S-7. Effect of the time of the recycling reaction, lysozyme concentration, 10^{-13} M

Principle of the DHM-SERS assay

DHM-SERS assay as a control experiment was carried out. To verify the feasibility of the designed THM, the DHM-SERS detection of lysozyme was conducted under the identical conditions. The sequence of the hairpin aptamer DNA is the same as that of the THM. The fundamental concept of this approach is illustrated in Scheme S-2. The DHM has two functional regions, aptamer region for target analyte recognition and the template of the signal probe replication. The SERS-DHM detection system consists of the DHM and SERS signal probe. With the cooperation of KF polymerases and Nb.BbvCI, this protocol can carry out the analysis of target through a two-cycle mode including target displacement recycling and DHM assisted strand-displacement polymerization, similar with the cycle 1 and cycle 2 of THM-SERS system. As illustrated in Scheme S-2, in the presence of lysozyme, the DHM is initiated to undergo structure switching via aptamer-target binding event. Thus two-cycle working mode is initiated by the DHM switch. After the execution of the whole network of DHM-SERS detection system, lysozyme as target analyte could be identified by measuring the Raman signal of SERS signal probe attached on MB. The signal is enhanced through accomplishing two-cycle amplification.

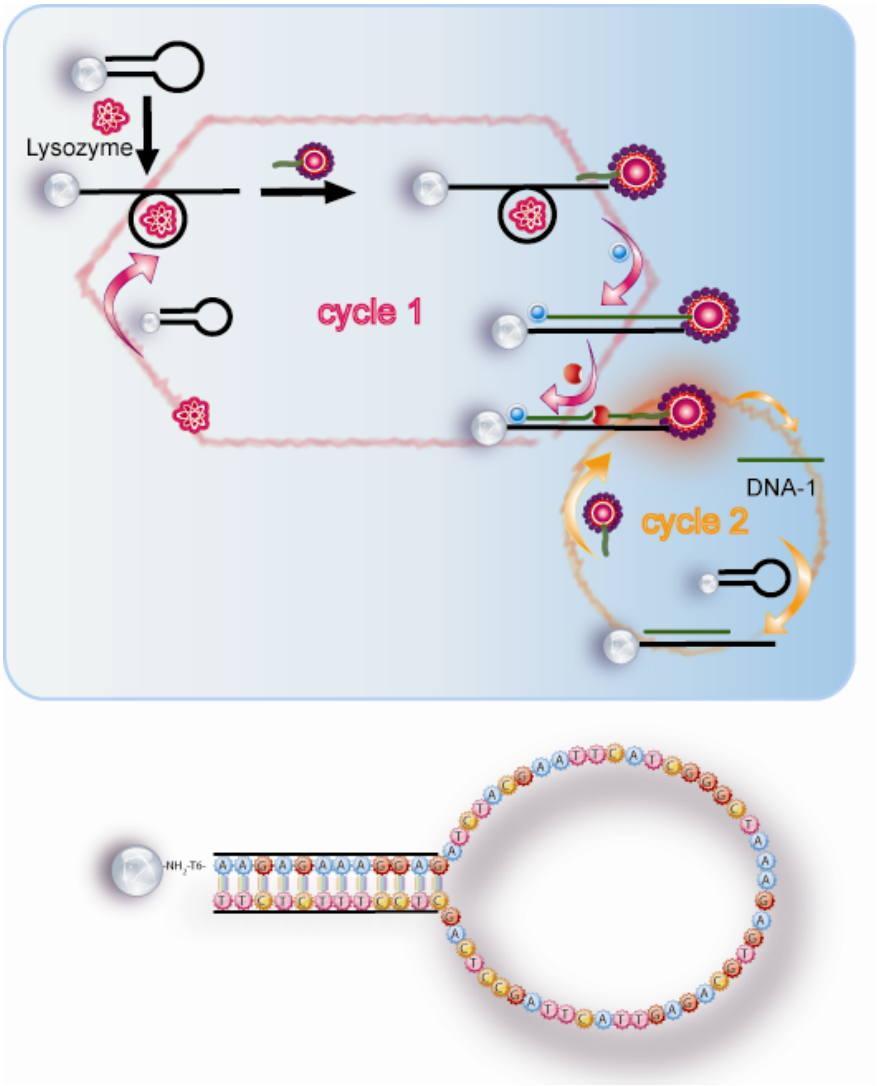

Scheme S-2. The schematic representation of the DHM-SERS assay.

Sensitivity of the DHM-SERS assay and comparison with the THM-SERS assay

The experiment was carried out with the DHM-SERS assay. As shown in Figure S-8, the normalized Raman intensity increased with the increase of the lysozyme concentration ranging from 1.0×10^{-14} to 1.0×10^{-11} M. The correlation equation is $\Delta I = 2.6443 \lg C + 38.9209$ (ΔI is the normalized Raman intensity subtracting the blank, C is the concentration of lysozyme, and R=0.9960). The detection limit of 6.3 fM was obtained (S/N=3). A relative standard deviation (RSD) of 7.2% was obtained by 11 replicate measurements of 1.0×10^{-12} M lysozyme, also showing a good reproducibility of the assay. However, the sensitivity of THM-SERS system was found to increase by about 1 order of magnitude compared with DHM-SERS system. In the THM-SERS system, the three-cycle mode amplification is triggered via the

target-aptamer binding event. However, in the DHM-SERS system, only the two-cycle mode reaction was initiated via the target-aptamer binding event Compared with DHM-SERS system, the amplification efficiency of the recycling mode is greatly enhanced in the THM-SERS system.

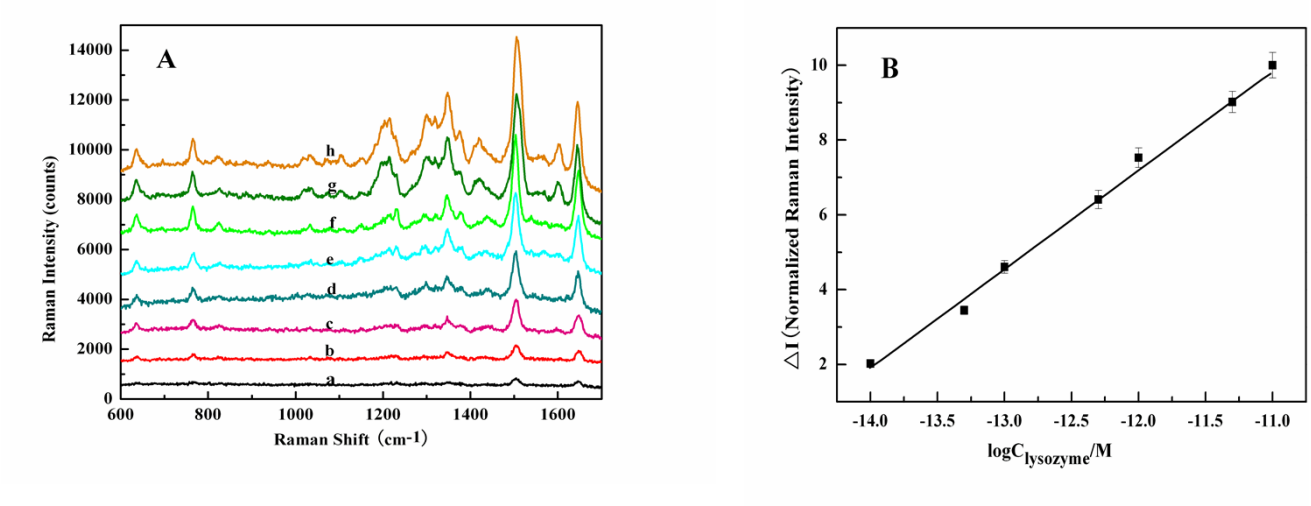

Figure S-8. (A) SERS spectra for increasing concentrations of lysozyme in the DHM-SERS system: a) 0, b) 1.0×10^{-14}, c) 5.0×10^{-14}, d) 1.0×10^{-13}, e) 5.0×10^{-13}, f) 1.0×10^{-12}, g) 5.0×10^{-12}, h) 1.0×10^{-11} M. (B) The variation of normalized Raman intensity with the concentration of lysozyme. The average of three spectra was obtained from different spots on the Au slides surface, and three repeated experiments were performed. Error bars showed the standard deviation of three experiments. The blank was subtracted for each value.

Specificity of the THM-SERS assay for the detection of lysozyme

The specificity of the SERS strategy was investigated and the corresponding results are shown in Figure S-9. The Raman response with several potential interferences was investigated. In the presence of BSA or thrombin at 10^{-10} M, no significant difference in SERS signals was obtained compared to the blank sample. However, the signal intensity for lysozyme was much larger even at its low concentration of 10^{-13} M. The experimental results demonstrated that the proposed method exhibited the high specificity for lysozyme detection.

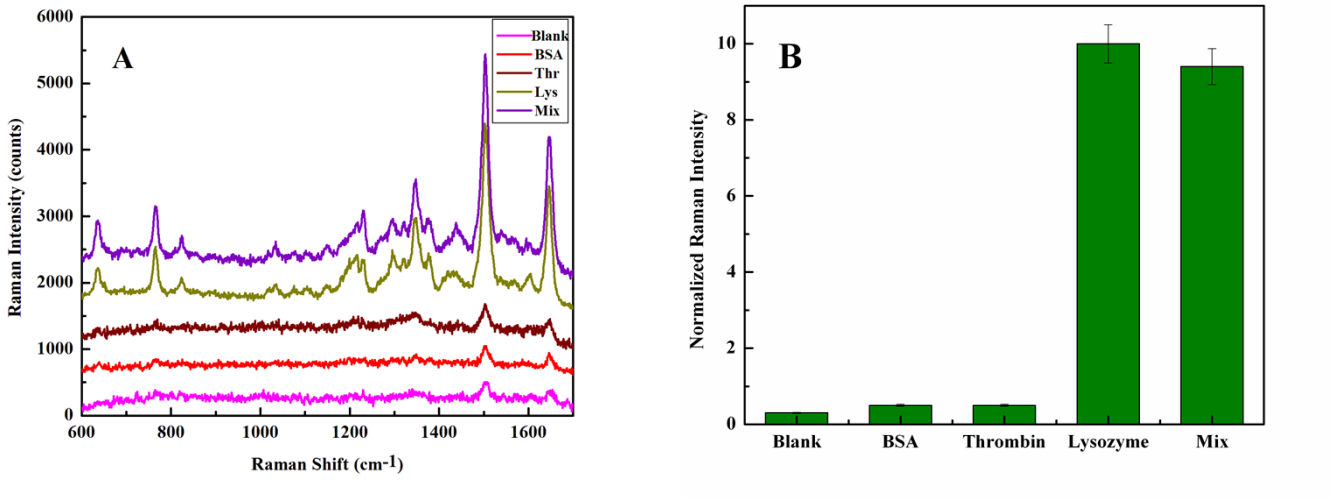

Figure S-9. Specificity for the detection of lysozyme against BSA and thrombin. The concentration of BSA and thrombin: 10^{-10} M, lysozyme concentration, 10^{-13} M. The blank was subtracted for each sample.

Real sample analysis of THM-SERS assay for lysozyme

To demonstrate the feasibility of the practical clinical analysis of the approach, the detection of lysozyme in human serum was investigated using standard addition calibration. Because of the high sensitivity and selectivity of this method, the serum sample was serially diluted before assay, then spiked with different amounts of lysozyme. After SERS measurement, the calibration method was used to determine lysozyme concentrations. The calculated content of lysozyme in human serum was 3.67×10^{-7} M, which was within the normal range of the previously reported values.[9] The recoveries obtained by comparing

the measured amounts to that of added lysozyme varied from 93.6 to 96.1% (Table S-3), suggesting that the SERS amplification strategy could be potentially applied for the detection of lysozyme in biologically relevant samples.

Scheme S-3

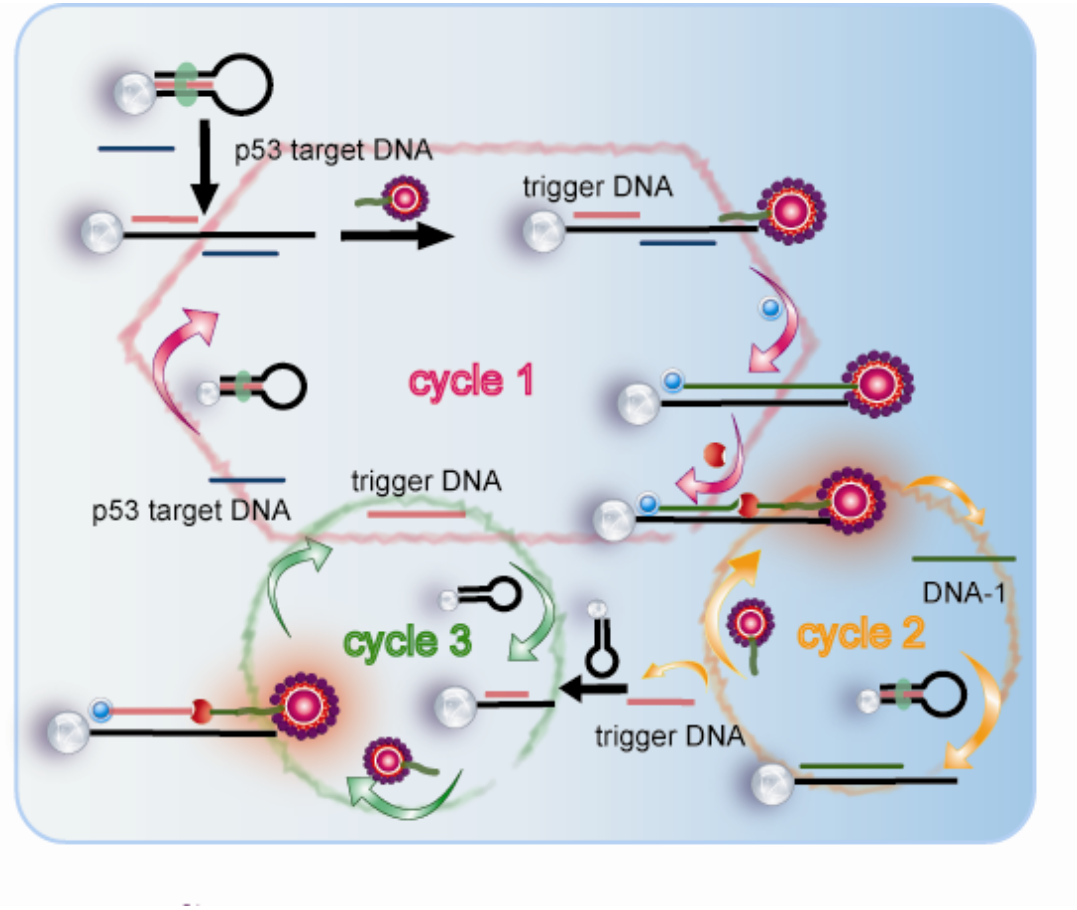

Scheme S-3. Schematic representation of the THM-SERS assay for p53 target DNA.

Sensitivity of the THM-SERS assay for the detection of p53 target DNA

In Figure S-10, the Raman response increased with the increase of the concentration of p53 target DNA in the range of 1.0×10^{-16} to 1.0×10^{-13} M. The correlation equation is $\Delta I = 2.6040 \lg C + 43.758$ (ΔI is the normalized Raman intensity subtracting the blank, C is the concentration of p53 target DNA, R = 0.9928). Obtained by 11 replicate measurements of 1.0×10^{-15} M p53 target DNA, RSD was 8.1%, showing excellent reproducibility. The detection limit of 21 aM was obtained (S/N=3). The comparison of different methods for p53 target DNA detection is shown in Table S-4 (ESI). The experiments of

selectivity and real blood sample detection are also shown in ESI (See detail in ESI, Figure S-10, Table S-5).

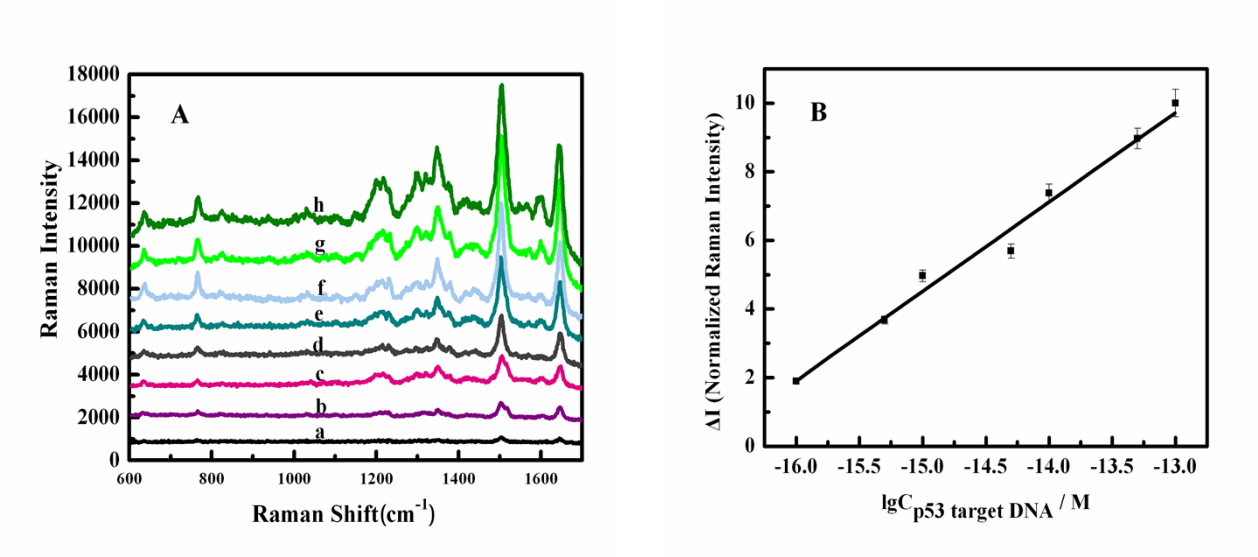

Figure S-10 (A) SERS spectra for increasing concentrations of p53 target DNA in the THM-SERS system: a) 0, b) 1.0×10^{-16}, c) 5.0×10^{-16} d) 1.0×10^{-15}, e) 5.0×10^{-15}, f) 1.0×10^{-14}, g) 5.0×10^{-14}, h) 1.0×10^{-13} M. (B) The variation of normalized Raman intensity with the concentration of p53 target DNA.

Specificity of the THM-SERS assay for the detection of p53 target DNA

To assess the selectivity of this method, the SERS intensity with probe A (non complementary DNA, column A), probe B (one base mismatched DNA, column B), p53 target DNA, (column C) and p53 target DNA in presence of 10^{-11} non complementary DNA, (column D) were presented in the concentrations of 10^{-15} M, 10^{-14} M, 10^{-13} M, respectively. In Figure S-11, it can be seen that in the presence of non complementary DNA, no significant difference in SERS signals was observed compared to the control group without p53 target DNA, suggesting that the THM is not triggered to open the hairpin structure. The SERS signal probe was not anchored on the MB. Accordingly to column B, the one-base mismatched DNA-1 produced a 60% lower analytical signal in comparison with the completely matched target DNA in the presence of 10^{-13} M. In addition, no obvious difference in the SERS intensity was observed for column C and column D, suggesting that the excess DNA has no significant effect on the detection of target DNA. The measured data demonstrated the high selectivity of the THM-SERS method for nucleic acid detection.

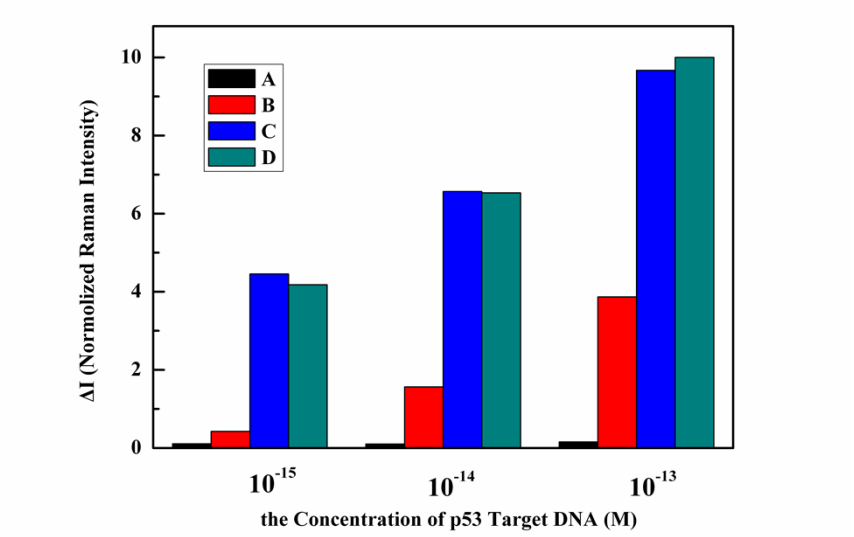

Figure S-11. Specificity for the detection of p53 target DNA against probe-A, probe B, p53 target DNA and p53 target DNA in presence of 10^{-11} M non complementary DNA, in the concentration respectively for 10^{-15} M, 10^{-14} M, 10^{-13} M. Normalized Raman intensity in presence of probe-A, column A, o probe-B, column B, target DNA 1 column C and target DNA in presence of 10^{-11} non complementary DNA, column D. The blank was subtracted for each value.

Real sample analysis of THM-SERS assay for the detection of p53 target DNA

The practical applicability of the THDM-SERS system was investigated by detecting p53 target DNA in a human real serum sample. The performance of p53 target DNA in a human real serum sample was investigated. The serum sample was spiked with different amounts of p53 target DNA. After SERS measurement, the recoveries obtained by comparing the measured amounts to that of added lysozyme varied from 86.3 to 92.6% (Table S-5). Three replicate determinations at different concentration levels exhibited RSDs ranging from 5.1 to 6.7% (n=3).

Table S-1.Oligonucleotide sequences used in this study

Oligonucleotides name	Sequences	Discription
Hairpin aptamer DNA in THM and DHM on MB	5'-NH_2-T_6-AAG AGA AAG GAG ATC TAC GAA TTC ATC AGG GCT AAA GAG TGC AGA GTT ACT TAG CCT CAG CTC CTT TCT CTT-3'	Underline means the lysozyme aptamer and the red region means a Nt. BbvCI recognition sequence in scheme 1
Trigger DNA	5'-TGAGG TTC TCT TTC CTC-3'	Single strand DNA formed the triplex structure
Duplex hairpin DNA	5'-NH_2-T_6-AAG AGA AAG GAG GAG GAA AGA GAA CCT CAG CTC CTT TCT CTT G-3'	The hairpin capture DNA immobilized on MB
Signal DNA	5'-Rox-TTT TTT CCT AGC GAC–SH–3'	Rox modified DNA immobilized on AuNPs for Raman signal
Capture DNA	5'-SH-CAAG AGA AAG GA-3'	The capture probe immobilized on AuNPs
Hairpin DNA in THDM	5'-NH_2-T_6-AAG AGA AAG GAG GGC ACA AAC ACG CAC CTC AA CCT CAG CTC CTT TCT CTT-3'	The hairpin DNA immobilized on MB in THDM-SERS system (underline means the sequence complementary to p53 target DNA)
P53 target DNA	5'-TTG AGG TGC GTG TTT GTG CC-3'	
Probe-A	5'–TTT TTT TTT TTT TTT TTT TT–3'	Non complementary DNA
Probe-B	5'-TTG AGG TAC GTG TTT GTG CC-3'	One base mismatched DNA recognition region (the red region means the mutant base)
Hairpin aptamer DNA	5'-/**FAM**/-AAG AGA AAG GAG ATC TAC GAA TTC ATC AGG GCT AAA GAG TGC AGA GTT ACT TAG CCT CAG CTC CTT TCT CTT-3'	Hairpin DNA formed the triplex structure modified with a fluorophore
Trigger DNA	5'-/**DABCYL**/-TTC TCT TTC CTC-3'	Single strand DNA formed the triplex structure with a quencher
DNA-1	5'-/**DABCYL**/-TGA CTC CTC AGA -3'	Non complementary DNA to THM with a quencher

Table S-2. Comparison of different methods for lysozyme detection.

Method	Transducer	Detection limit
The reduced aggregation of perylene probe	Fluorescence	70 pM [10]
The aggregation of quantum dots triggered by protein	Resonant light scattering	3 nM[11]
The signal amplification on DNA machine	Electrochemistry	0.52 pM[12]
Aptamer−gold nanoparticle conjugates	Colorimetry	16 nM[13]
Signal amplification on multiple cycle amplification strategy	SERS	1 fM[14]
Acidified-sulfate-induced aggregation	SERS	350 nM [15]
The competition-mediated pyrene-switching aptasensor	Fluorescence	200 pM[16]
The aggregation of magnetic nanoparticle conjugated with lysozyme aptamer	Magnetic relaxation switch	0.5 nM[17]
Aptamer DNAzyme hairpin structures	Colorimetry	0.5 pM[18]
The adsorption of DNA/protein complex on carbon nanotubes	Luminescence	0.9 nM[19]
Signal amplification on self-assembly of DNAzyme aptamer conjugate	Chemiluminescence	0.1 pM[20]
This method	DHM-SERS method THM-SERS method	6.3 fM 0.54 fM

Table S-3. Recovery of lysozyme assay in human serum samples

Nos.	Lysozyme content added	Lysozyme content detected	Recovery (%)	RSD (%)
1	5.0×10^{-15} M	4.76×10^{-15} M	95.2%	6.3%
2	1.0×10^{-14} M	9.61×10^{-15} M	96.1%	5.7%
3	5.0×10^{-14} M	4.68×10^{-14} M	93.6%	6.5%

Table S-4. Comparison of different methods for p53 target DNA detection

Method	Transducer	Detection limit
Signal amplification on toehold-mediated strand displacement reaction	Quartz crystal microbalance	0.3 nM [21]
Gold nanorods used as both colorimetric probe and fluorescence quencher.	Colorimetry Fluorescence	0.3 nM 0.26 pM[22]
A catalytic colorimetric assay assisted by nicking endonuclease signal amplification	Colorimetry	1 pM[23]
Signal amplification on circular common target molecule displacement polymerization	Fluorescence	80 pM[24]
A self-assembled DNA nanostructure on the hybridization chain reaction	Quartz crystal microbalance with dissipation monitoring	0.1 nM[25]
Intermolecular G-quadruplex integrated sticky-end pairing assembly based colorimetric system	Colorimetry	0.2 nM[26]
Electrochemical methylation-specific ligation detection reaction	Electrochemistry	300 pM[27]
This method	SERS	21 aM

Table S-5. Recovery of p53 target DNA assay in human serum samples

Nos.	P53 target DNA content added	P53 target DNA content detected	Recovery (%)	RSD (%)
1	5.0×10^{-16} M	4.45×10^{-16} M	89.0%	5.1%
2	1.0×10^{-15} M	8.63×10^{-14} M	86.3%	5.9%
3	5.0×10^{-15} M	4.63×10^{-15} M	92.6%	6.7%

References

[1] G. Frens, *Nat. Phys. Sci.* **1973,** *241,* 20-22.

[2] K. C. Grabar, P. C. Smith, M. D. Musick, J. A. Davis, D. G. Walter, M. A. Jackson, A. P. Guthrie, M. J. Natan, *J. Am. Chem. Soc.* **1996,** *118,* 1148-1153.

[3] T. A. Taton, C. A. Mirkin, R. L. Letsinger, *Science* **2000,** *289,* 1757-1760.

[4] S. J. Ye, Y. X. Yang, J. Xiao, S. S. Zhang, *Chem. Commun.* **2012,** *48,* 8535-8537.

[5] S. S. Zhang, Y. M. Yan, S. Bi, *Anal. Chem.* **2009,** *81,* 8695-8701.

[6] A. K. R. Lytton-Jean, M. Han, S. C. A. Mirkin, *Anal. Chem.* **2007,** *79,* 6037-6041.

[7] S. J. Ye, H. X. Li, W. Cao, *Biosens. Bioelectron.* **2011,** *26*, 2215-2220.

[8] T. Nguyen, M. B. Francis, *Organic Letters* **2003,** *5,* 3245-3248.

[9] M. A. Mir, *Postgrad. Med. J.* **1977,** *53,* 257-259.

[10] B. Wang, C. Yu, *Angew. Chem. Int. Ed.* **2010,** *49,* 1485-1488.

[11] P. Wu, T. Zhao, Y. F. Tian, L. Wu, X. D. Hou, *Chem. Eur. J.* **2013,** *19,* 7473-7479.

[12] H. Zhang, C. C. Fang, S. S. Zhang, *Chem. Eur. J.* **2011,** *17,* 7531-7537.

[13] B-H. Kim, I. S. Yoon, J-S. Lee, *Anal. Chem.* **2013,** *85,* 10542-10548.

[14] P. He, Y. Zhang, L. J. Liu, W. P. Qiao, S. S. Zhang, *Chem. Eur. J.* **2013,** *19,* 7452-7460.

[15] X. X. Han, G. G. Huang, B. Zhao, Y. Ozaki, *Anal. Chem.* **2009,** *81,* 3329-3333.

[16] J. Huang, Z. Zhu, S. Bamrungsap, G. Z. Zhu, M. X. You, X. X. He, K. M. Wang, W. H. Tan, *Anal. Chem.* **2010,** *82,* 10158-10163.

[17] S. Bamrungsap, M. I. Shukoor, T. Chen, K. Sefah, W. H. Tan, *Anal. Chem.* **2011,** *83,* 7795-7799.

[18] C. Teller, S. Shimron, I. Willner, *Anal. Chem.* **2009,** *81,* 9114-9119.

[19] X. Y. Ouyang, R. Q. Yu, J. Y. Jin, J. S. Li, R. H. Yang, W. H. Tan, J. L. Yuan, *Anal. Chem.* **2011,** *83,* 782-789.

[20] D. Li, B. Shlyahovsky, J. Elbaz, I. Willner, *J. Am. Chem. Soc.* **2007,** *129,* 5804-5805.

[21] D. Z. Wang, W. Tang, X. J. Wu, X. Y. Wang, G. J. Chen, Q. Chen, N. Li, and F. Liu, *Anal. Chem.* **2012,** *84,* 7008-7014.

[22] W. H. Wang, Y. N. Zhao, Y. Jin, ACS *Appl. Mater. Interfaces.* **2013,** *5,* 11741-11746.

[23] Z. Y. Lin, W. Q. Yang, G. Y. Zhang, Q. D. Liu, B. Qiu, Z. W. Cai, G. N. Chen, *Chem. Commun.,* **2011,** *47,* 9069-9071.

[24] L. P. Qiu, Z. S. Wu, G. L. Shen, R. Q. Yu, *Anal. Chem.* **2011***, 83,* 3050-3057.

[25] W. Tang, D. Z. Wang, Y. Xu, N. Li, F. Liu, *Chem. Commun.,* **2012,** *48,* 6678-6680.

[26] H. B. Li, Z-S. Wu, Z. F. Shen, G. L . Shen, R. Q.Yu, *Nanoscale***,2014,** *6,* 2218-2227.

[27] Z. Dai, T. Cai, W. Y. Zhu, X. Y. Gao, X. Y. Zou, *Chem. Commun.,* **2013,** *49*, 1939-1941.